Carpathian Journal of Earth and Environmental Sciences, August 2020, Vol. 15, No. 2, p. 405 – 413; Doi:10.26471/cjees/2020/015/140

COMPARISON OF RUSLE AND SUPERVISED CLASSIFICATION ALGORITHMS FOR IDENTIFYING EROSION-PRONE AREAS IN A MOUNTAINOUS RURAL LANDSCAPE

Kwanele PHINZI[1*], Njoya Silas NGETAR[2], Osadolor EBHUOMA[3] & Szilárd SZABÓ[4]

[1]Doctoral School of Earth Sciences, Department of Physical Geography and Geoinformatics, University of Debrecen, Egyetem tér 1., Debrecen H-4032, Hungary, e-mail: phinzi.kwanele@science.unideb.hu
[2]School of Agricultural, Earth and Environmental Sciences, University of KwaZulu-Natal, Howard College Campus, Durban 4041, South Africa, e-mail: njoya@ukzn.ac.za
[3]School of Agricultural, Earth and Environmental Sciences, University of KwaZulu-Natal, Westville Campus, Durban 4000, South Africa, e-mail: osadolorebhuoma@gmail.com
[4]Department of Physical Geography and Geoinformatics, University of Debrecen, Egyetem tér 1., Debrecen H-4032, Hungary, e-mail: Szabo.szilard@science.unideb.hu

Abstract: The identification of erosion prone areas with reasonably high accuracy is a prerequisite for formulating relevant soil conservation measures especially in rural areas where there is much reliance on subsistence agriculture. The aim of this paper was to compare and exploit the complementary advantage of fusing three independent methods including the Revised Universal Soil Loss Equation (RUSLE) and two supervised image classification algorithms: Random Forest (RF) and Maximum Likelihood (ML). All analyses were conducted using a GIS proprietary software, ArcGIS. The results indicated that RF was the best with the highest overall accuracy (OA), producer's accuracy (PA), and user's accuracy (UA) of 87%, 78%, and 95%, respectively. RUSLE poorly performed relative to other methods, scoring the lowest PA (34%) and OA (66%), but slightly outperformed ML in terms of UA. From the user's perspective, the performance of individual methods was satisfactory with each method achieving an UA of greater than 90% although ML and RUSLE were not satisfactory from the producer's perspective, recording respective PAs of 56% and 34%. When the results from individual methods were fused, the accuracy increased above 90% across all accuracy indices, which is far above the 85% acceptable level for planning and management purposes.

Keywords: RUSLE, supervised classification, random forest, maximum likelihood, soil erosion

1. INTRODUCTION

Soil erosion is among the most detrimental forms of land degradation and has attracted considerable attention worldwide (Lal, 2001; Morgan, 2005; Dragićević et al., 2010; FAO, 2019; Tošić et al., 2019). Soil erosion affects the crops growth and yield by removing the fertile top soil, incorporating denser subsoil into the surface layer, and by potentially decreasing the rooting zone of the soil (Van Oost & Bakker, 2012). These effects have serious implications for sustainable agriculture (Phinzi & Ngetar, 2017; Rodrigo-Comino et al., 2018; Waltner et al., 2018), and environemtal safety (Ştefănescu et al., 2011). Sediement accumulation resulting from erosion is equally detrimental (Jordan et al., 2005; Yang et al., 2011), reducing the quality and quantity of water (Phinzi et al., 2020a).

The importance of information on areas endangered by erosion cannot be emphasised enough, especially if sustainable agriculture is to be realised in rural communities (Farsang et al., 2012; Cristofari et al., 2017). Due to its simplicity and consideration of many erosion factors, the Revised Universal Soil Loss Equation (RUSLE), an empirical erosion model proposed by Renard et al., (1997), remains one of the most widely used methods for assessing erosion in various parts worldwide. This widespread usage of RUSLE can be partly attributed to improved computer processing power and advances in geospatial technologies such as remote sensing (Phinzi & Ngetar, 2019a), which have facilitated erosion assessment at

limited costs and with reasonable accuracies (Wang et al., 2003).

Apart from the above-mentioned advantages, remote sensing can identify erosion prone areas through image classification. Many classification algorithms exist, ranging from supervised Maximum Likelihood (ML), Minimum Distance to Mean (MDM), parallelepiped, Random Forest (RF), and Support Vector Machines (SVM), Multivariate Adaptive Regression Splines (MARS) to unsupervised K-means and Iterative Self Organising DATa Analysis (ISODATA) (Lo Curzio & Magliulo, 2010; Wickama et al., 2015; Cheng et al., 2018; Mustafa et al., 2018; Rotigliano et al., 2018; Gayen et al., 2020). Among these algorithms, RF and ML algorithms have become a popular choice for image classification in the last few years. The popularity of RF is mainly due to its flexibility as it can be used for both classification and regression purposes and can handle both categorical and continuous variables (Breiman, 2001; Rodriguez-Galiano et al., 2012; Woznicki et al., 2019). Owing to such flexibility, RF has been used in many application areas like: identification of roofing material (Abriha et al., 2018), soil erosion risk mapping (Cheng et al., 2018), lithological classification (Ge et al., 2018), land use/land cover mapping (Monteiro et al., 2017; Szabó, et al., 2019), and gully extraction (Phinzi et al., 2020a). On the other hand, ML is a statistical-based algorithm that uses probability density functions to describe the distribution of pixels within land cover classes and assigns them to the class with the highest likelihood (Bolstad & Lillesand, 1991; Ahmad & Quegan, 2012). Like RF, the ML algorithm has been widely used in a range of applications. In land use/land cover, the performance of RF against that of ML and/or other algorithms has been evaluated based on remotely sensed data (Noi & Kappas, 2018; Abdi, 2019).

Although studies comparing RF and ML are common, from the perspective of soil erosion, however, very few studies use these algorithms in conjunction with empirical erosion models like RUSLE. Specifically, the possibility of integrating RF, ML, and RUSLE as independent methods for identifying erosion prone areas remains unexplored until recently. Phinzi et al., (2020b) integrated RUSLE and RF to analyse the spatial pattern of soil erosion risk, focusing on soil loss and influencing erosion factors. Cheng et al., (2018) introduced a RF-based approach that integrates remotely sensed and ancillary data to map soil erosion risk distribution. These studies provided the basis for further exploration of empirical erosion models and supervised image classification algorithms in erosion assessment, with specific emphasis on their complementary advantages. In this study, we evaluate the performance of RUSLE, RF, and ML in terms of erosion classification accuracy. Unlike previous attempts, however, herein, we evaluate the accuracy of the selected methods both individually and when combined. Furthermore, we report a fourth method, called here "multi-classifier", which takes a full complementary advantage of the three methods. Rather than simple averaging the accuracy (i.e. overall accuracy) values of individual methods, the three methods are spatially fused and the accuracy of the resulting output (multi-classifier) is assessed independently. Increasingly, emphasis is being placed on combining different classification techniques to obtain better classification results. This is evident in recent studies such as that of Dong et al., (2020) which fused RF and Convolutional Neural Network (CNN) algorithms. However, studies using remote sensing data with machine learning usually concentrate on land cover classification or vegetation density calculation (Nomalised Difference Vegetation Index - NDVI) as one factor of the soil erosion model (e.g. Suriyaprasit & Shrestha, 2008; Nyesheja et al. 2019; Atoma et al., 2020). Research on the use of machine learning as a direct tool or merged with other methods to detect erosion prone areas is still limited. Therefore, the main aim of this study is to fuse RUSLE, an empirical erosion model, with RF and ML algorithms.

2. MATERIALS AND METHODS

2.1. Study area

The study area has a surface area of about 382 km2 and is in the Eastern Cape Province of South Africa (Fig. 1). The reason for selecting this study area relates to the fact that it is arguably one of the most hard-hit areas by water erosion. Gullies, rills, and piping (subsurface erosion) are prevalent in the area. The area is predominantly rural with the majority of inhabitants involved in subsistence agriculture (Phinzi & Ngetar, 2019b). Presently, the most common land use types include scattered rural settlements, rangeland grazing, and dryland agriculture. Mudstone and sand stone of the Beaufort Group characterise the geology of the area (Hilbich et al., 2007). The topography of the study area is generally steep, particularly in the western and some northern parts, with an elevation range of 890 m to 2015 m. The annual rainfall is 671mm and temperatures range from 7 ºC to 30 ºC. The study area is drained by Umzintlava River as the major river.

The climate is semiarid with four seasons: Autumn (March May), Winter (June–August), Spring (September–November) and Summer (December–February).

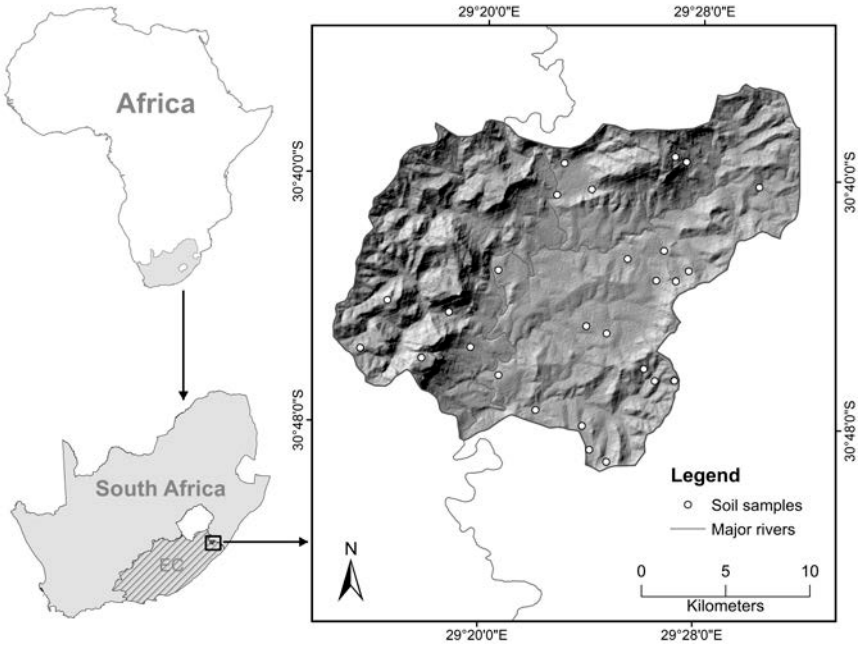

Figure 1. Location of study area in the Eastern Cape (EC) Province, South Africa

2.2. Data acquisition

Datasets acquired from different sources consisted of monthly rainfall, Digital Elevation Model (DEM), soil samples, and Systeme Pour l'Observation de la Terre (SPOT-7) image. The monthly rainfall data spanning a period of 46 years (1970 – 2016) was obtained from the South African Weather Services (SAWS). The Shuttle Radar Topography Mission (SRTM) DEM, with a vertical accuracy of 16 m and spatial resolution of 30 m, was downloaded from the USGS website. Soil data consisting of 24 soil samples were collected from the topsoil layer (0 – 30cm). Soil samples were air-dried and analysed in the laboratory to determine soil erodibility factors (i.e. particle size, soil organic matter, structure and permeability).

The SPOT-7 image, with a spatial resolution of 5.5 m for multispectral bands (Blue, Green, Red, and Near Infrared) and 1.5 m for panchromatic band, was obtained from the South African National Space Agency (SANSA). These data were used as input in the computation of RUSLE parameters using various equations (Table 1). These equations were selected based on the availability of data, objectives and characteristics of the study area (Phinzi & Ngetar, 2019b).

2.3. Pre-processing

Radiometric correction was performed on SPOT-7 image using the image analysis module in ArcMap. We applied the Apparent Reflectance function to convert the SPOT-7 Digital Numbers (DNs) to top of atmosphere (TOA) reflectance values. This function also corrects the effects caused by solar irradiance and zenith angle (Cui et al., 2014).

In order to maintain uniformity and minimise spatial errors, datasets from various sources were co-registered to a common coordinate system, Universal Traverse Mercator (UTM zone 35S) based on World Geodetic System (WGS 1984) (Phinzi et al., 2020b). Additionally, a standard cell size of 5.5 m for RUSLE parameters was used.

2.4. Revised Universal Soil Loss Equation (RUSLE)

RUSLE computes the average annual soil loss based on the multiplication of five erosion factors including rainfall (R-factor), soil type (K-factor), topography (LS-factor), cover management (C-factor), and support practice (C-factor). In this study, all these erosion factors were computed in ArcMap and used to calculate the average annual soil loss based on equation 1 (Renard et al., 1997):

$$A = R \times K \times LS \times C \times P \quad (1)$$

Where A is the average annual soil loss ($t\ ha^{-1}yr^{-1}$), R is the rainfall erosivity ($MJ\ mm.\ ha^{-1}h^{-1}yr^{-1}$), K is the soil erodibility ($t\ J^{-1}mm^{-1}$), LS is the slope length and slope steepness, C is the cover and management, and P is the support practice. The LS, C, and P factors are dimensionless. Many equations are available for calculating RUSLE factors and the ones used in this study are shown in Table 1. As a computerised method, RUSLE is compatible with Geographic Information System (GIS). This makes it

Table 1. Equations used to calculate RUSLE parameters in this study

Parameter	Formula	Input data	Source
R	$R = \sum_{i=1}^{12} 1.735\ x\ 10^{(1.5log\frac{p_i^2}{p} - 0.8188)}$ Where R represents rainfall erosivity, p_i represents the total monthly precipitation (mm), and p is the mean annual precipitation (mm) (Wischmeier and Smith, 1978).	Rainfall data	SAWS http://www.weathersa.co.za/
K	$K = 2.77 \times 10^{-7}(12 - OM)M^{1.14} + 4.28 \times 10^{-3}(s - 2) + 3.29 \times 10^{-3}(p - 3)$ $M = [(Sil + vFSa) \times (100 - Cla)]$ Where K is the soil erodibility factor (t h $MJ^{-1}mm^{-1}$), OM is the soil organic matter content (%), Sil is the silt fraction (%), vFSa is the very fine sand fraction (%), Cla is the clay fraction (%), S is a soil structure code, P is a permeability class (Rosewell, 1993).	Soil samples	Primary data
LS	$LS = (\frac{A}{22.13})^m \times (\frac{sin\beta}{0.0896})^n$ $A = (\text{Flow accumulation} \times \text{Cell value})$ Where LS is the slope length and slope steepness (dimensionless), A is the upslope contributing area per unit cell (m), m (0.4) is a variable slope length exponent, n (1.3) is a slope steepness exponent (Moore & Burch, 1986).	SRTM DEM	USGS https://earthexplorer.usgs.gov/
C	$C = exp^{\left(-a\frac{NDVI}{(\beta - NDVI)}\right)}$ Where C represents the cover and management factor (dimensionless), a (2) and β (1) are the parameters that determine the shape of the NDVI curve (Van der Knijff et al., 2000).	SPOT-7 image	SANSA https://www.sansa.org.za/
P	$P = 0.2 + 0.03 \times S$ Where P is the support practice factor (dimensionless), and S is the slope (%) (Wener (1981).	SRTM DEM	USGS https://earthexplorer.usgs.gov

SRTM (Shuttle Radar Topography Mission), DEM (Digital Elevation Model), SPOT (*Systeme Pour l'Observation de la Terre*), SAWS (South African Weather Services), USGS (United states Geological Survey), SANSA (South African National Space Agency).

easy to integrate RUSLE with other geographically referenced data and conduct analysis within a single digital environment.

In order to delineate eroded areas using RUSLE, we first generated an erosion risk map, consisting of six erosion risk classes including "very low", "low, moderate", "high", "very high", and "extremely high" (Bergsma et al., 1996). Second, we then reclassified this map into two classes, viz. erosion (moderate to extremely high risk) and non-erosion classes (i.e. very low to low risk) (Phinzi et al., 2020b).

2.5. Random Forest (RF)

RF is a supervised machine learning algorithm developed to overcome the instability of traditional tree-based methods (Breiman, 2001). RF consists of a set of decision trees, each tree contributing a single vote to a classification (Adelabu & Dube, 2015). The final classification outcome is determined by the majority vote. Depending on the software used to run the algorithm, two RF parameters need to be optimised, i.e. ntree (the number of trees) and mtry (the number of features in a split).

We ran RF classification using the Sentinel Application Platform (SNAP) toolbox (http://step.esa.int). After experimenting with different ntree values (e.g. 10, 20, 30, 40, 50), we used the default value (as the simplest model) as the differences in the classification outcome and overall accuracy were negligible. As the first step towards identifying erosion prone areas, we trained the

algorithm on seven land cover classes (i.e. water bodies, built-up areas, barren land, soil erosion, agricultural land, rangeland, and forest). These land cover classes were defined following a USGS-based classification system (Anderson et al., 1976). We used all the original input bands of SPOT-7. Second, we reclassified the land cover map into erosion and non-erosion (Phinzi et al., 2020b). In other words, only those pixels belonging to soil erosion land cover class were classified as erosion whereas pixels belong to other land cover classes were classified as non-erosion.

2.6. Maximum Likelihood (ML)

ML, a supervised parametric algorithm initially proposed by German mathematician C.F. Gauss in 1821 for normal distribution (Ge et al., 2018), is by far the most commonly used classification method in remote sensing (Richards & Xiuping, 2006). The algorithm is implemented quantitatively to consider several classes and several spectral bands simultaneously (Campbell & Wynne, 2011). ML assumes that the probability density function for each class is multivariate and assigns an unknown pixel to a class with the highest probability of membership, thus, the name maximum likelihood (Scott & Symons, 1971; Bolstad & Lillesand, 1991). As a common multivariate statistical classification algorithm, ML is embedded in many image processing software packages, we conducted the classification using the SNAP toolbox (Ge et al., 2018). We followed the same procedure used for classifying soil erosion with RF (Section 2.5).

2.7. Fusion of different methods

Different methods (RUSLE, RF, and ML) were combined on a cell-by-cell basis. This was achieved using the "Cell Statistics", a spatial analyst tool available in ArcGIS software. The tool calculates a per-cell statistics (e.g. mean, sum, range, standard deviation etc.) from different raster inputs as given by equation 2 (ArcGIS 10.4). We selected sum as an overlay statistic.

$$OutRas = InRas1 + InRas2 + InRas3 \quad (2)$$

Where OutRas is the output raster, InRas1, 2 and 3 are input rasters corresponding to RUSLE, RF and ML, respectively. We called the resulting output raster "multi-classifiers".

2.8. Ground truth data collection and accuracy assessment

Field observations and high resolution Google Earth images were used to collect ground truth data. We collected 800 random (400 erosion and 400 non-erosion) points as ground truth data and divided the data into a training set in 75-25%.

We used the confusion matrix to assess the accuracy of the classified erosion as is the most widely accepted method, providing overall accuracy (OA), kappa coefficient and class-specific accuracies like producer's accuracy (PA) and user's accuracy (UA) (Congalton, 1991; Lillesand et al., 2015). The OA and kappa coefficient are the two most popular accuracy indices used in assessing remote sensing-derived classifications (Noi & Kappas, 2018). For comparative evaluation of the three methods (e.g. ML, RF, and RUSLE), we used OA, PA, and UA in our study.

3. RESULTS AND DISCUSSION

The results of soil erosion derived from ML and RF were slightly the same whereas RUSLE-based results differed considerably compared to these two algorithms (Table 2, Fig. 2). Results indicated that RUSLE only considered steep sloping areas, most notably, in the western and northern parts of the study area. It can be observed that in the central and other areas where the elevation was relatively gentle, RUSLE completely missed soil erosion. Of the three methods, ML had the most pixels (798671) classified as erosion (Table 2)

Table 2. Eroded area in the study region as determined by different methods

Method	Pixel	Area (km^2)	Area (%)
ML	798671	24.16	6.32
RF	655312	19.82	5.19
RUSLE	143152	4.33	1.13

These pixels translate to an area of approximately 24 km2 (6%) in the real world. Following ML, RF and RUSLE-classified soil erosion covered an area of about 20 km2 (5%) and 4 km2 (1%), respectively. Fig. 3 shows one of the severely eroded sites in the study area.

The accuracy assessment results showed that all three methods generally performed well at least in terms of UA, scoring above 90% (Table 3). Across all accuracy assessment indices, RF outperformed other methods, recording 87%, 78%, and 95% on OA, PA, and UA, respectively. These results are in line with findings from other studies where RF performed better than other methods. For instance, Burai et al., (2015) showed that machine learning methods including RF

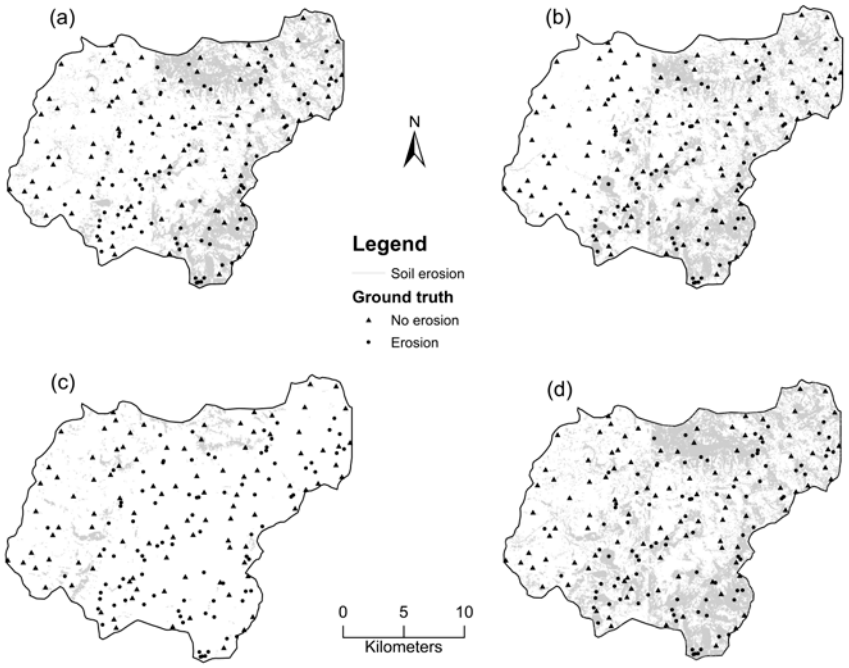

Figure 2. Soil erosion distribution from different classification methods: (a) ML, (b) RF, (c) RUSLE, and (d) multi-classifiers. Note: circle (erosion) and triangle (no erosion) represent ground truth points

achieved higher accuracies compared to ML. Recently, superior classification performance of RF over RUSLE was reported (Phinzi et al., 2020b).

However, there are instances where ML outperformed RF. An example is the lithological classification study in which ML was the best classifier, providing the highest classification accuracy (more than 70%) compared to RF and Artificial Neural Network (ANN) which both scored less than 70% (Ge et al., 2018). In our study however, the ML algorithm performed poorer relative to RF, achieving an OA of 76%. Of the three methods, RUSLE recorded the lowest OA (66%) and PA (34%) but performed better than ML based on UA (94%). Based on the recommended 85% and 70% classification for OA and class-specific accuracies, respectively (Anderson et al., 1976; Everitt et al., 2008), it is apparent that the performance of ML and RUSLE was not satisfactory. This discrepancy in the classification results of individual methods underscores the importance of fusing different methods.

Figure 3. Severely eroded area in the study area

When all the three methods were combined, the OA and PA improved considerably (i.e. greater than 90%). Nevertheless, the combined output (multi-classifier) did not result in any improvement in RF and RUSLE's UAs except for ML's UA which improved from 92% to 94%. However, the results from the combined output are still satisfactory as they average above 90% which is far higher than 85%

Table 3. Accuracy assessment for classified soil erosion (note: overall accuracy (OA), producer's accuracy (PA), and user's accuracy (UA)

Method	OA	PA	UA
ML	76%	56%	92%
RF	87%	78%	95%
RUSLE	66%	34%	94%
Multi-classifiers	93%	91%	94%

threshold set as satisfactory for planning and management purposes (Anderson et al., 1976; Mohammady et al., 2015). As a conservation planning tool, RUSLE is reputed to show the accurate patterns of erosion (Smith, 1999), but its accuracy greatly decreases (as was the case in this study) in complex landscapes characterised by steep topography and severely gullied areas. Hence, the need for developing a robust methodology combining advanced classification algorithm and RUSLE.

4. CONCLUSIONS

The aim of this study was to evaluate the performance of three methods (i.e. ML, RF, and RUSLE) in soil erosion classification. The results indicated that different methods achieved different accuracy levels. RF performed better than other methods across all accuracy indices. RUSLE obtained lowest accuracy values but performed better than ML at least with respect to UA. The combined output from the three methods resulted in considerably high levels of accuracy, recording above 90% across all indices (OA, UA, and PA). These results reinforce the importance of fusing empirical erosion models and machine learning algorithms in erosion assessment, which so far has not received much attention. Soil erosion varies from one region to another, depending on the socio-economic and environmental factors at play in a particular region, thus the result may vary as well. Further research needs to be conducted in different locations. Preferably, in addition to RUSLE, RF, and ML, various other empirical erosion models and machine learning and/or deep learning algorithms need to be considered in future erosion assessments.

Acknowledgement

The research was supported by the Thematic Excellence Programme of the Ministry for Innovation and Technology in Hungary (ED 18-1-2019-0028), within the framework of the Space Sciences thematic programme of the University of Debrecen.

REFERENCES

Abdi, **A**.**M**., 2019. *Land cover and land use classification performance of machine learning algorithms in a boreal landscape using Sentinel-2 data*. GIScience & Remote Sensing, 57, 1, 1-20.

Abriha, **D**., **Kovács**, **Z**., **Ninsawat**, **S**., **Bertalan**, **L**., **Balázs**, **B**. & **Szabó**, **S**., 2018. *Identification of roofing materials with Discriminant Function Analysis and Random Forest classifiers on pan-sharpened WorldView-2 imagery–a comparison*. Hungarian Geographical Bulletin, 67,4, 375-392.

Adelabu, **S**. & **Dube**, **T**., 2015. *Employing ground and satellite-based QuickBird data and random forest to discriminate five tree species in a Southern African Woodland*. Geocarto International, 30,4, 457-471.

Ahmad, **A**. & **Quegan**, **S**., 2012. *Analysis of maximum likelihood classification on multispectral data*. Applied Mathematical Sciences, 6, 129-132, 6425-6436.

Anderson, **J**.**R**., **Hardy**, **E**.**E**., **Roach**, **J**.**T**. & **Witmer**, **R**.**E**., 1976. *A land use and land cover classification system for use with remote sensor data*. Geological Survey Professional Paper 964, U.S. Government Printing Office, Washington DC.

Atoma, **H**., **Suryabhagavan**, **K**.**V**., & **Balakrishnan**, **M**., 2020. *Soil erosion assessment using RUSLE model and GIS in Huluka watershed, Central Ethiopia*. Sustainable Water Resources Management, 6,1, 12.

Bergsma, **E**., **Charman**, **P**., **Gibbons**, **F**., **Hurni**, **H**., **Moldenhauer**, **W**.**C**. & **Panichapong**, **S**., 1996. *Terminology for soil erosion and conservation*. ISSS: ITC: ISRIC.

Bolstad, **P**. & **Lillesand**, **T**.**M**., 1991. *Rapid maximum likelihood classification*. Photogrammetric Engineering and Remote Sensing, 57, 1, 67-74.

Breiman, **L**., 2001. *Random forests*. Machine Learning, 45, 1, 5-32.

Burai, **P**., **Deák**, **B**., **Valkó**, **O**. & **Tomor**, **T**., 2015. *Classification of herbaceous vegetation using airborne hyperspectral imagery*. Remote Sensing, 7, 2, 2046-2066.

Campbell, **J**.**B**. & **Wynne**, **R**.**H**., 2011. *Introduction to remote sensing*. Guilford Press. 5th edition, New York, 718 p.

Cheng, **Z**., **Lu**, **D**., **Li**, **G**., **Huang**, **J**., **Sinha**, **N**., **Zhi**, J. & **Li**, **S**., 2018. *A random forest-based approach to map soil erosion risk distribution in Hickory Plantations in western Zhejiang Province, China*. Remote Sensing, 10, 12, 1899.

Congalton, **R**.**G**., 1991. *A review of assessing the accuracy of classifications of remotely sensed data*. Remote Sensing of Environment, 37, 1, 35-46.

Cristofari, **H**., **Girard**, **N**. & **Magda**, **D**., 2017. *Supporting transition toward conservation agriculture: a framework to analyze the learning processes of farmers*. Hungarian Geographical Bulletin, 66, 1, 65-76.

Cui, **L**., **Li**, **G**., **Ren**, **H**., **He**, **L**., **Liao**, **H**., **Ouyang**, **N**. & **Zhang**, **Y**., 2014. *Assessment of atmospheric correction methods for historical Landsat TM images in the coastal zone: A case study in Jiangsu, China*. European Journal of Remote Sensing, 47, 1, 701-716.

Dong, **L**., **Du**, **H**., **Mao**, **F**., **Han**, **N**., **Li**, **X**., **Zhou**, **G**., **Zhu**, **D**., **Zheng**, **J**., **Zhang**, **M**., **Xing**, **L**., & **Liu**, **T**., 2020. *Very High Resolution Remote Sensing Imagery Classification Using a Fusion of Random Forest and Deep Learning Technique—Subtropical Area for Example*. IEEE Journal of Selected Topics in Applied Earth Observations and Remote Sensing, 13, 113-128.

Dragićević, **S**., **Nenadović**, **S**., **Jovanović**, **B**., **Milanović**, **M**., **Novković**, **I**., **Pavić**, **D**., & **Lješević**, **M**., 2010. *Degradation of Topciderska river water quality (Belgrade)*. Carpathian Journal of Earth and Environmental Sciences, 5, 2, 177-184.

Everitt, **J**. **H**., **Yang**, **C**., **Fletcher**, **R**. & **Deloach**, **C**.**J**., 2008. *Comparison of QuickBird and SPOT 5 satellite imagery for mapping giant reed*. Journal of Aquatic Plant Management, 46, 77-82.

FAO. 2019., *Soil erosion: the greatest challenge to sustainable soil management*. Rome, 100 p.

Farsang, **A**., **Kitka**, **G**., **Barta**, **K**., & **Puskas**, **I**., 2012. *Estimating element transport rates on sloping agricultural land at catchment scale (Velence mts., NW Hungary)*. Carpathian Journal of Earth and Environmental Sciences, 7, 4, 15-26.

Gayen, **A**., **Haque**, **S**. **M**., & **Saha**, **S**., 2020. *Modeling of Gully Erosion Based on Random Forest Using GIS and R*. In Gully Erosion Studies from India and Surrounding Regions (pp. 35-44). Springer, Cham.

Ge, **W**., **Cheng**, **Q**., **Tang**, **Y**., **Jing**, **L**. & **Gao**, **C**., 2018. *Lithological classification using sentinel-2A data in the Shibanjing ophiolite complex in inner Mongolia, China*. Remote Sensing, 10, 4, 638.

Hilbich, **C**., **Daut**, **G**., **Mäusbacher**, **R**., & **Helmschrot**, **J**., 2007. *A landscape-based model to characterize the evolution and recent dynamics of wetlands in the Umzimvubu headwaters, Eastern Cape, South Africa*. Wetlands: Monitoring, Modelling and Management, 61.

Jordan, **G**., **Van Rompaey**, **A**., **Szilassi**, **P**., **Csillag**, **G**., **Mannaerts**, **C**., & **Woldai**, **T**., 2005. *Historical land use changes and their impact on sediment fluxes in the Balaton basin (Hungary)*. Agriculture, ecosystems & environment, 108,2, 119-133.

Lal, **R**., 2001. *Soil degradation by erosion*. Land Degradation & Development, 12(6), 519-539.

Lillesand, **T**., **Kiefer**, **R**.**W**. & **Chipman**, **J**.**W**., 2015. *Remote sensing and image interpretation*. John Wiley & Sons, 7th edition, New York, 768 p.

Lo Curzio, **S**., & **Magliulo**, **P**., 2010. *Soil erosion assessment using geomorphological remote sensing techniques: an example from southern Italy*. Earth Surface Processes and Landforms: The Journal of the British Geomorphological Research Group, 35,3, 262-271.

Mohammady, **M**., **Moradi**, **H**.**R**., **Zeinivand**, **H**. & **Temme**, **A**.**J**.**A**.**M**., 2015. *A comparison of supervised, unsupervised and synthetic land use classification methods in the north of Iran.* International Journal of Environmental Science and Technology, 12, 5, 1515-1526.

Monteiro, **A**.**T**., **Gonçalves**, **J**., **Fernandes**, **R**. **F**., **Alves**, S., **Marcos**, **B**., **Lucas**, **R**., ... & **Honrado**, **J**. **P**., 2017. *Estimating invasion success by non-native trees in a national park combining WorldView-2 very high resolution satellite data and species distribution models*. Diversity, 9, 1, 6.

Moore, **I**.**D**. & **Burch**, **G**.**J**., 1986. *Physical Basis of the Length-slope Factor in the Universal Soil Loss Equation 1*. Soil Science Society of America Journal, 50, 5, 1294-1298.

Morgan, **R**.**P**.**C**., 2005. *Soil Erosion and Conservation*, Blackwell. Oxford, 3rd edition.

Mustafa, **M**.**R**.**U**., **Sholagberu**, **A**.**T**., **Yusof**, **K**.**W**., **Hashim**, **A**.**M**., **Khan**, **M**.**W**.**A**., & **Shahbaz**, **M**., 2018. *SVM-Based Geospatial Prediction of Soil Erosion Under Static and Dynamic Conditioning Factors*. In MATEC Web of Conferences (Vol. 203, p. 04004).

Noi, **T**.**P**. & **Kappas**, **M**., 2018. *Comparison of random forest, k-nearest neighbor, and support vector machine classifiers for land cover classification using Sentinel-2 imagery*. Sensors, 18, 1, 18.

Nyesheja, **E**.**M**., **Chen**, **X**., **El-Tantawi**, **A**.**M**., **Karamage**, **F**., **Mupenzi**, **C**., & **Nsengiyumva**, **J**.**B**., 2019. *Soil erosion assessment using RUSLE model in the Congo Nile Ridge region of Rwanda*. Physical Geography, 40,4, 339-360.

Phinzi, **K**. & **Ngetar**, **N**. **S**., 2019a. *The assessment of water-borne erosion at catchment level using GIS-based RUSLE and remote sensing: A review*. International Soil and Water Conservation Research, 7, 1, 27-46.

Phinzi, **K**. & **Ngetar**, **N**.**S**. & **Ebhuoma**, **O**., 2020b. *Soil erosion risk assessment in the Umzintlava Catchment (T32E), Eastern Cape, South Africa, using RUSLE and random forest algorithm*. South African Geographical Journal, 1-25.

Phinzi, **K**. & **Ngetar**, **N**.**S**., 2017. *Mapping soil erosion in a Quaternary catchment in Eastern Cape using Geographic information system and remote sensing*. South African Journal of Geomatics, 6, 1, 11-29.

Phinzi, **K**. & **Ngetar**, **N**.**S**., 2019b. *Land use/land cover dynamics and soil erosion in the Umzintlava catchment (T32E), Eastern Cape, South Africa*. Transactions of the Royal Society of South Africa, 74, 3, 223-237.

Phinzi, **K**., **Abriha**, **D**., **Bertalan**, **L**., **Holb**, **I**., & **Szabó**, **S**. 2020a. *Machine Learning for Gully Feature Extraction Based on a Pan-Sharpened Multispectral Image: Multiclass vs. Binary Approach*. ISPRS International Journal of Geo-Information, 9, 4, 252.

Renard, **K**.**G**., **Foster**, **F**.**G**., **Weesie**s, **G**.**A**., **McCool**, **D**.**K**. & **Yoder**, **D**.**C**., 1997. *Predicting soil erosion by water: a guide to conservation planning with the Revised Universal Soil Loss Equation (RUSLE)*. US Department of Agriculture, Washington, DC.

Richards, **J**.**A**. & **Xiuping**, **J**., 2006. *Remote sensing digital image analysis.* Springer, 4th edition, Berlin, 494 p.

Rodrigo-Comino, **J**., **Neumann**, **M**., **Remke**, **A**. & **Ries**, **J**. **B**. 2018. *Assessing environmental changes in abandoned German vineyards. Understanding key issues for restoration management plans*. Hungarian Geographical Bulletin, 67, 4, 319-332.

Rodriguez-Galiano, **V**. **F**., **Ghimire**, **B**., **Rogan**, **J**., **Chica-Olmo**, **M**. & **Rigol-Sanchez**, **J**.**P**., 2012. *An*

assessment of the effectiveness of a random forest classifier for land-cover classification. ISPRS Journal of Photogrammetry and Remote Sensing, 67, 93-104.

Rosewell, **C**.**J**., 1993. *SOILOSS: a program to assist in the selection of management practices to reduce erosion*. Technical handbook No. 11, Sydney: Conservation Services of New South Wales, Department of Conservation and Land Management.

Rotigliano, **E**., **Martinello**, **C**., **Agnesi**, **V**., & **Conoscenti**, **C**., 2018. *Evaluation of debris flow susceptibility in El Salvador (CA): a comparison between Multivariate Adaptive Regression Splines (MARS) and Binary Logistic Regression (BLR)*. Hungarian Geographical Bulletin, 67,4, 361-373.

Scott, **A**. **J**. & **Symons**, **M**. **J**., 1971. *Clustering methods based on likelihood ratio criteria*. Biometrics, 27, 2, 387-397.

Smith, **H**.**J**., 1999. *Application of empirical soil loss models in southern Africa: A review*. South African Journal of Plant and Soil, 16, 3, 158-163.

Ştefănescu, **L**., **Constantin**, **V**., **Surd**, **V**., **Ozunu**, **A**., & **Vlad**, **Ş.** N., 2011. *Assessment of soil erosion potential by the USLE method in Roşia Montană mining area and associated natech events*. Carpathian Journal of Earth and Environmental Sciences, 6,1, 35-42.

Suriyaprasit, **M**., & **Shrestha**, **D**.**P**., 2008. *Deriving land use and canopy cover factor from remote sensing and field data in inaccessible mountainous terrain for use in soil erosion modelling*. The international archives of the photogrammetry, remote sensing and spatial information sciences, 37,PartB7, 1747-1750.

Szabó, **L**., **Burai**, **P**., **Deák**, **B**., **Dyke**, **G**. **J**. & **Szabó**, **S**., 2019. *Assessing the efficiency of multispectral satellite and airborne hyperspectral images for land cover mapping in an aquatic environment with emphasis on the water caltrop (Trapa natans)*. International Journal of Remote Sensing, 40, 13, 5192-5215.

Tošić, **R**., **Lovrić**, **N**., & **Dragićević**, **S**., 2019. *Assessment of the impact of depopulation on soil erosion: case study–Republika Srpska (Bosnia and Herzegovina)*. Carpathian Journal of Earth and Environmental Sciences, 14, 2, 505-518.

Van der Knijff, **J**.**M**.**F**., **Jones**, **R**.**J**.**A**. & **Montanarella**, **L**., 2000. *Soil erosion risk assessment in Italy. European Soil Bureau, European Commission*, pp. 32.

Van Oost, **K**. & **Bakker**, **M**.**M**. 2012., *Soil productivity and erosion*. In D. H. Wall, R. D. Bardgett, V. Behan Pelletier, J. E. Herrick, H. Jones, K. Ritz, J. Six, D. R. Strong, & W H. van der Putten, eds. Soil ecology and ecosystem services, Oxford University Press, Oxford, 301-314 p.

Waltner, **I**., **Pásztor**, **L**., **Centeri**, **C**., **Takács**, **K**., **Pirkó**, **B**., **Koós**, **S**., & **László**, **P**., 2018. *Evaluating the new soil erosion map of Hungary—A semiquantitative approach*. Land Degradation & Development, 29, 4, 1295-1302.

Wang, **G**., **Gertner**, **G**., **Fang**, **S**. & **Anderson**, **A**.**B**., 2003. *Mapping multiple variables for predicting soil loss by geostatistical methods with TM images and a slope map*. Photogrammetric Engineering & Remote Sensing, 69, 8, 889-898.

Wener, **C**.**G**., 1981. *Soil Conservation In Kenya, Nairobi*. Ministry of Agriculture, Soil Conservation Extension Unit.

Wickama, **J**., **Masselink**, **R**., & **Sterk**, **G**., 2015. *The effectiveness of soil conservation measures at a landscape scale in the West Usambara highlands, Tanzania*. Geoderma, 241, 168-179.

Wischmeier, **W**.**H**. & **Smith**, **D**.**D**., 1978. *Predicting rainfall erosion losses-a guide to conservation planning. Predicting rainfall erosion losses-a guide to conservation planning*. USDA Agricultural Handbook, No. 537.

Woznicki, **S**.**A**., **Baynes**, **J**., **Panlasigui**, **S**., **Mehaffey**, **M**. & **Neale**, **A**., 2019. *Development of a spatially complete floodplain map of the conterminous United States using random forest*. Science of the Total Environment, 647, 942-953.

Yang, **S**. **L**., **Milliman**, **J**.**D**., **Li**, **P**., & **Xu**, **K**., 2011. *50,000 dams later: erosion of the Yangtze River and its delta*. Global and Planetary Change, 75,1-2, 14-20.

Received at: 08. 06. 2020
Revised at: 12. 08. 2020
Accepted for publication at: 14. 08. 2020
Published online at: 17. 08. 2020